

Retraction notice

Optimization of CO₂ Gas Flow rate and Distributor Holes Number for CO₂ Capture

Nuryoto Nuryoto*, Leli Rahmawati and Herliza Julvita

Chemical Engineering Department, Faculty of Engineering, Universitas Sultan Ageng Tirtayasa, Cilegon, Banten, Indonesia

Rafiif Nur Tahta Bagaskara

School of Environment, Faculty of Arts and Science, University of Toronto, Toronto, Canada

* Corresponding author. E-mail: nuryoto@untirta.ac.id DOI: 10.14416/j.asep.2025.000007

Received: 9 June 2025; Revised: 23 July 2025; Accepted: 7 August 2025; Published online: 16 September 2025

© 2025 King Mongkut's University of Technology North Bangkok. All rights Reserved.

Abstract

The chemical reaction between CO₂ and Ca(OH)₂ to produce precipitated calcium carbonate (PCC) occurs optimally when effective interaction between the two reactants takes place. The interaction between reactants will affect the reaction rate and conversion of reactants (CO₂ and Ca(OH)₂) into the PCC products. Among the parameters that influence the interaction of CO₂ gas with the Ca(OH)₂ solution are the CO₂ gas flow rate and the numbers of CO₂ gas distributor holes. Therefore, this study aims to analyze and understand the phenomena involved, specifically how variations in CO₂ gas flow rate and the numbers of distributor holes affect the performance of CO₂ capture based on the resulting precipitated calcium carbonate (CaCO₃). The research was conducted using a semi-batch reactor, stirring speed of 400 rpm, hydrostatic pressure of 9.8 kPa, CO₂ gas flow rate of 2–5 liters per minute (lpm), and the numbers of distributor holes ranging from 3 to 9. The results of the observation showed that the effect of increasing CO₂ gas flow rate and the numbers of distributor holes to enhance the interaction between reactants in the reaction system has its optimal condition. The optimal condition was obtained at a CO₂ gas flow rate of 3 lpm and the number of 6 holes, with a resulting PCC (CaCO₃) product of 39.02 grams.

Keywords: Carbon dioxide, Diffusion, Global warming, Reaction, Semi-batch, Solution

1 Introduction

Chemical reaction can be simply defined as the transformation of a compound (reactant) into a new compound (product) that is different from the original compound. In chemical reactions involving 2 or more reactants to form certain products, interaction between the reactants is required, because without interaction, the reaction process will not occur. Good interaction between reactants will impact the reaction rate and the extent of conversion of reactants into the resulting reaction products. Theoretically, interaction between reactions can occur well when the diffusion process between reactants occurs without obstacle, allowing the diffusion-reaction process to proceed quickly [1]. The diffusion-reaction process between reactants (CO₂ and Ca(OH)₂) can be illustrated as shown in Figure 1 [1],

[2]. Another factor influencing the diffusion-reaction in gas-liquid systems is the solubility factor [3]–[5]. The solubility of gas plays an important role because the amount of CO₂ gas bubbles that diffuse and react is influenced by the amount of CO₂ dissolved in the Ca(OH)₂ solution. The more CO₂ gas that is dissolved, the more PCC product will be produced. The solubility correlation, referring to Mutailipu *et al.* [4] related to the solubility of CO₂ gas in the solution (in the form of water) and simplified referring to Smith *et al.* [6], can be expressed with Equation (1).

$$y_{CO_2}P = H_{CO_2} \cdot x_{CO_2} \quad (1)$$

with, y_{CO_2} = molar fraction of CO₂ in gas phase (dimensionless), x_{CO_2} = molar fraction of CO₂ in

liquid phase (dimensionless), and H_{CO_2} = Henry constant CO_2 (Pa), and P = system pressure (Pa)

In Equation (1), it can be seen that the solubility of CO_2 is influenced by the pressure of CO_2 gas, where if the reaction system is carried out at a certain pressure and the CO_2 gas flow rate (V_{CO_2}) is increased, it has the potential to increase the molar fraction of dissolved CO_2 (x_{CO_2}). On the other hand, increasing the CO_2 gas flow rate will increase the number of moles of CO_2 (n_{CO_2}) introduced into the solution (see Equation (2)), and will result in an increase in the molar fraction of dissolved CO_2 ($x_{CO_2} = \frac{n_{CO_2}}{n_{H_2O} + n_{CO_2}}$). The correlation between the gas flow rate (V_{CO_2}) and the moles of CO_2 (n_{CO_2}) can be explained by Equation (2) [6].

$$PV_{CO_2} = z n_{CO_2} R T \quad (2)$$

with, z = compressibility factor of CO_2 (dimensionless), n_{CO_2} = mol CO_2 (mol), T = Temperature (K), P = pressure (Pa), V_{CO_2} = volume of CO_2 (m^3), R = universal gas constant ($Pa \cdot m^3 / mol \cdot K$)

Another way to increase the amount of dissolved CO_2 gas in the reaction system is by increasing the number of CO_2 gas bubbles that will come into

contact, thereby increasing the potential for CO_2 gas to dissolve and diffuse, as presented in Equation (3) [1], [7].

$$\frac{dn_N}{dt} = -D \frac{dC_{CO_2}}{\delta} \quad (3)$$

with, D = diffusivity coefficient (m^2/s), dC_{CO_2} = difference in CO_2 concentration that passes through the film layer (mol/m^3), δ = film layer (m), $\frac{dn_N}{dt}$ = molar diffusion rate with a certain number of bubbles ((mol/s), N = number of bubbles (dimensionless).

So, when the number of CO_2 gas bubbles is increased, the potential for the gas bubbles to diffuse and react will be greater. The diffusion and reaction process occurs steadily, meaning the diffusion rate will be the same as the reaction rate, thus Equation (4) applies [1]

$$D \frac{dC_{CO_2}}{\delta} = k C_{CO_2} C_{Ca(OH)_2} \quad (4)$$

with, k = reaction rate constant ($m^3/(mol \cdot s)$), C_{CO_2} = concentration of CO_2 that reacts (mol/m^3), and $C_{Ca(OH)_2}$ = concentration of $Ca(OH)_2$ that reacts (mol/m^3), $D \frac{dC}{\delta}$ = diffusion rate ($mol/(m^2 \cdot s)$) and $k C_{CO_2} C_{Ca(OH)_2}$ = reaction rate ($mol/(m^2 \cdot s)$).

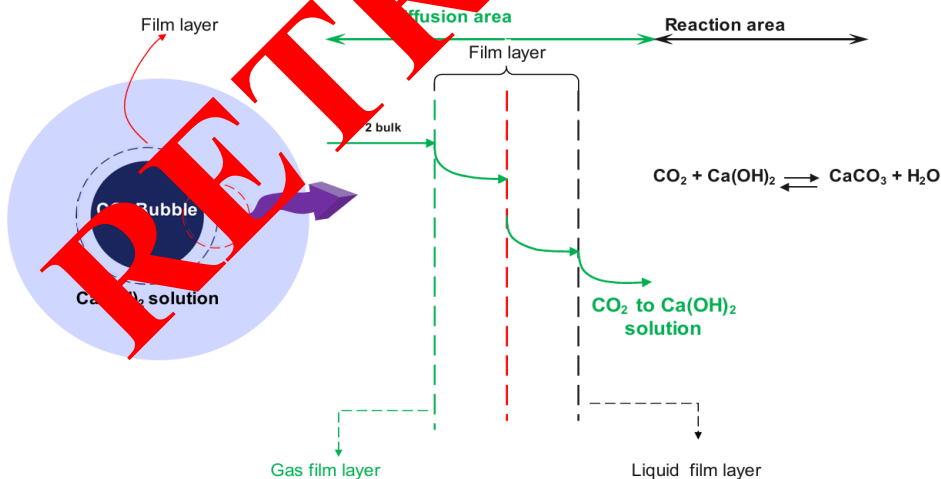
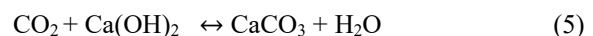
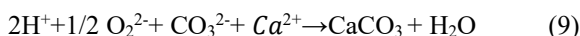
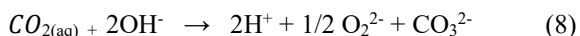
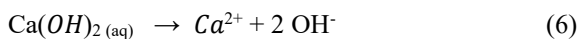


Figure 1: Illustration of the diffusion-reaction process of CO_2 gas and $Ca(OH)_2$ solution into PCC ($CaCO_3$) [1], [8], [9].

Stoichiometrically, the reaction between CO_2 and $Ca(OH)_2$ to form PCC ($CaCO_3$) and water (H_2O) can be written as in Equation (5) [10].



The reaction illustrated in Equation 5 is further explained in Equations (6) to (9).



Studies related to the synthesis of PCC using the carbonation method, which involves reacting CO₂ gas and Ca(OH)₂, have been extensively conducted by previous researchers. Several previous studies have explored CO₂ capture using Ca(OH)₂ solutions through various operational methods. For example, the use of CaO and water with the addition of aloe vera extract as an additive achieved a precipitated calcium carbonate (PCC) formation efficiency of 91–93% at reaction temperatures ranging from 30 to 100 °C and a CO₂ flow rate of 1 L/min. [10]. Another study combined stirring with variations in reaction temperature (30–85 °C) and a CO₂ flow rate of 2–2.3 L/min, resulting in the predominance of calcite crystals along with minor amounts of vaterite or aragonite [11], [12]. Variations in Ca(OH)₂ concentration (0.2–0.35 M) have also been examined, showing CO₂ capture efficiencies of up to 90% with calcite and vaterite as the main crystalline phases [13]. An alternative approach used a 2.5 M sodium glycinate solution added to Ca(OH)₂, yielding a Ca(OH)₂ to CaCO₃ conversion rate of 96.5%, with calcite crystals accounting for approximately 93% of the product [14]. Meanwhile, studies conducted at high temperatures (200 °C) with very high gas flow rates reported a CO₂ capture efficiency of only 25% [15]. These studies have contributed to a solid understanding of CO₂ capture using Ca(OH)₂ based absorbents under various conditions. However, to date, no research has specifically evaluated the combined effect of the number of distributor holes and the CO₂ gas flow rate on capture performance in an integrated manner. This is a critical gap, as most prior studies have investigated these variables in isolation. In reality, the interaction between CO₂ flow rate and distributor hole configuration could significantly affect the gas-liquid contact area, gas residence time, and pressure stability, which are key parameters in optimizing carbonation reactor performance and improving capture efficiency. The objective of this study is to analyze and understand the underlying

phenomena, particularly how variations in CO₂ flow rate and the number of distributor holes influence the performance of CO₂ capture, as indicated by the formation of PCC. The findings are expected to complement previous research and serve as a foundational reference for developing carbon capture, utilization, and storage (CCUS) technologies that are more effective, efficient, and economically viable for industrial scale applications.

2 Materials and Methods

2.1 Material and Equipment

The raw material used in this research was a calcium hydroxide (Ca(OH)₂) solution obtained from CV. Kasugian Jaya, Cilegon, Banten – Indonesia, with a concentration of 15% (w/w) and categorized as technical grade. The CO₂ gas used was purified CO₂ (purity 99.9%) classified as technical grade, and was supplied by PT Gasindo Andalan Sukses, Cilegon, Banten, Indonesia. All chemicals were used as received without further purification. The research equipment is illustrated in Figure 2.

2.2 Research procedure

The pipe was filled with water up to a height of 100 cm, equivalent to a hydrostatic pressure of 9.8 kPa [9], [16]. The next step was to add 200 mL of Ca(OH)₂ solution into the reactor and run the stirrer at a speed of 400 rpm. CO₂ gas was flowed by adjusting the regulator with a flow rate of 2–5 lpm (liters/minute) through the predetermined number of distributor holes (3–9 holes), with a hole size of 0.2 cm and system temperature of 30 °C [9],[16]. When the reaction process reached the specified interaction time of 60 minutes, the reaction was stopped. The next step was to separate the PCC product precipitate from the reaction using filter paper, then dry it in an oven at 110 °C for 2 hours. The dried PCC powder was weighed to determine the amount of PCC produced for each observed variable [9], [16]. In addition, the obtained PCC powder was characterized through Fourier Transform Infrared (FTIR) testing to ensure that the reaction between the reactants (CO₂ and Ca(OH)₂) indeed occurred and Scanning Electron Microscope (SEM) testing to determine the surface morphology of the PCC crystals formed to ascertain the type of PCC produced (calcite, aragonite, vaterite, or a mixture of the three).

The mass of PCC produced from the reaction process conducted in each observed variable is calculated using Equation (10).

$$W_{PCC} = W_k - W_s \quad (10)$$

With, W_{PCC} = mass of PCC (grams), W_k = mass of filter paper + PCC product (grams), W_s = mass of filter paper (grams).

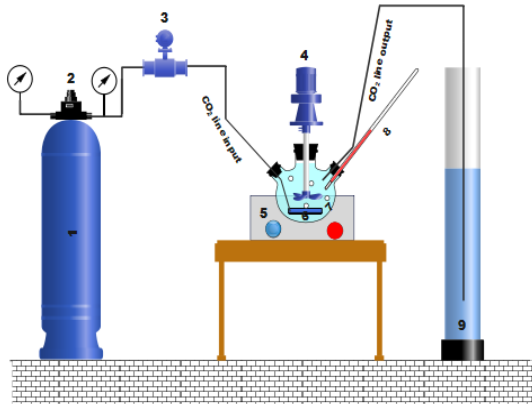


Figure 2: Research equipment schematic: (1) CO₂ gas cylinder, (2) gas regulator, (3) flow meter, (4) overhead magnetic stirrer, (5) heating mantle, (6) three-holes gas distributor, (7) three-neck flask, (8) thermometer, and (9) water tank.

3 Results and Discussion

3.1 Effect of CO₂ gas flow rate

In Figure 3, increasing the CO₂ gas flow rate into the reaction system does not always have a positive impact on the yield of the product PCC as described in Equations (1) and (2), but beyond a certain flow rate, it actually has a negative impact. When the CO₂ gas flow rate was increased from 2 to 3 lpm, the amount of PCC produced increased from 12.1 to 23.22 grams (an increase of 91.90%). The opposite condition

occurred when the CO₂ gas flow rate was increased from 3 to 5 lpm, resulting in a decrease in the amount of PCC produced, from 23.22 to 18.23 grams (a decrease of 21.49%). This phenomenon occurred because when the CO₂ gas flow rate was increased to 5 lpm, significant turbulence occurred, causing the Ca(OH)₂ solution to be lifted, and visually, a lot of Ca(OH)₂ suspension was seen sticking to the surface of the reactor walls (three-neck flask). This condition resulted in a decrease in the contact between CO₂ gas and Ca(OH)₂, as the amount of Ca(OH)₂ in the solution decreased, leading to a reduction in the reaction rate, which was also followed by a decrease in the amount of PCC produced. A similar phenomenon was also observed by previous researchers (see Table 1). As shown in Table 1, increasing the CO₂ gas flow rate within a specific range led to a decline in CO₂ capture performance, as indicated by a decrease in capture efficiency. This outcome is theoretically sound, as once a gas-liquid absorption system reaches its maximum capacity, any further increase in CO₂ flow rate results in a reduced residence time for the gas (see Equation 11). This reduction in residence time negatively impacts the contact duration between the gas and the absorption

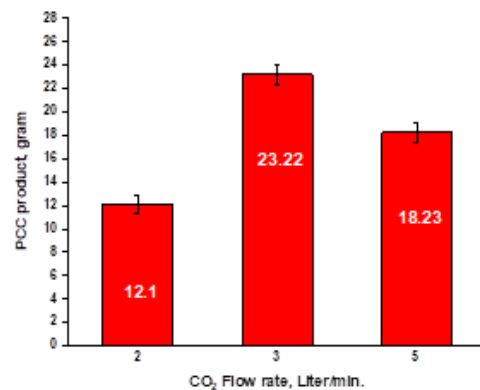


Figure 3: Effect of CO₂ gas flow rate with 3 distributor holes.

Table 1: Effect of CO₂ gas flow rate on CO₂ capture performance.

CO ₂ Capture	CO ₂ Flow Rate	Study Result	Ref.
Using a 5 w% NaOH solution with a flow rate of 180 mL/min.	7.6 – 24.7 L/min.	The CO ₂ capture efficiency dropped significantly from 90.2% to 41%.	[17]
Using Mono Ethanol Amine (MEA), piperazine (PZ), and ethylenediamine (EDA) with a flow rate of 200 ml/min.	100–800 mol/min.	CO ₂ capture efficiency decreased as the gas flow rate increased. For the PZ absorbent, efficiency dropped from 95% to 60%, while MEA and EDA showed declines from 95% to 40% and 30%, respectively.	[18]
Using Ca(OH) ₂ absorbent with a bubble absorption system, with an absorbent flow rate of 200 ml/min.	0.5 – 0.9 L/min.	CO ₂ capture experienced a decline, with resulting CO ₂ removal efficiencies recorded consecutively at 38, 36, 35, 33, and 31%	[19]

$$\tau = \frac{V_t}{\vartheta_{CO_2}} \quad (11)$$

Where, τ = residence time (minutes), V_t = column or reactor volume (dm^3), and ϑ_{CO_2} = CO_2 flow rate ($dm^3/minute$).

The flow velocity of CO_2 gas in the carbonation process (Equation (11)) fundamentally has a dual effect on CO_2 capture. On one hand, it enhances mass transfer; on the other, it can potentially reduce the reaction rate. Increased turbulence caused by higher CO_2 gas velocity (ϑ_{CO_2}) improves gas-liquid mixing, thereby enhancing the diffusion-reaction process (see Equation (4)) [20]. However, when the CO_2 gas velocity becomes too high, it can negatively impact the CO_2 capture process by reducing the residence time, which decreases the interaction between CO_2 and $Ca(OH)_2$ in the solution. This reduction in contact time ultimately lowers the overall CO_2 capture performance [21]. Therefore, there is a tradeoff between the benefits of increased turbulence, which enhances diffusion, and the drawback of reduced residence time. If the gas flow rate is too high, the loss in efficiency due to shorter residence time may outweigh the benefits, resulting in a reduced amount of CO_2 reacting with $Ca(OH)_2$ to form PCC. This outcome is reflected in Figure 3 and Table 1.

Referring to Figure 1, the phenomenon that occurs with the increase in CO_2 flow rate in the CO_2 capture process using $Ca(OH)_2$ can be illustrated as shown in Figure 4.

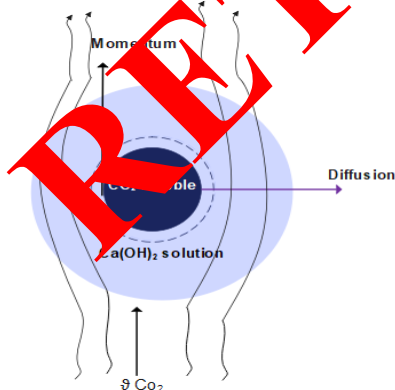


Figure 4: Illustration of the impact of gas flow rate on CO_2 capture.

As shown in Figure 4, an increase in CO_2 gas flow rate (ϑ_{CO_2}) leads to an increase in CO_2 gas momentum. When this momentum increase significantly exceeds the diffusion rate of CO_2 bubbles

into the $Ca(OH)_2$ solution, it results in reduced residence time and shorter contact duration between CO_2 and $Ca(OH)_2$. For example, based on the reactor volume of 300 mL, the residence time decreases from 0.15 minutes (at 2 L/min) to 0.10 minutes (at 3 L/min), and further to 0.06 minutes (at 5 L/min). Consequently, the performance of the CO_2 capture process declines.

3.2 The influence of the number of distributor holes

The increase in the number of CO_2 gas distributor holes had a similar tendency to the CO_2 gas flow rate variable, where the PCC production increased and then decreased (see Figure 5). An increase in the number of distributor holes from 3 to 6 resulted in a notable improvement in PCC production, increasing from 23.22 grams to 35.92 grams. This result is consistent with the theoretical principles described in Equations (3) and (4). Under stable CO_2 pressure and system conditions, increasing the number of distributor holes led to a higher number of CO_2 bubbles (N), as well as adjustments in bubble size, while maintaining steady bubble motion. Under these conditions, the concentration gradient of CO_2 in the $Ca(OH)_2$ solution (dC_{CO_2}) increased, thereby enhancing the diffusion rate of CO_2 into the solution, as described in Equation (3). This enhancement subsequently increased the reaction rate between CO_2 and $Ca(OH)_2$ in the solution, in accordance with Equation (4) and as illustrated in Figure 1. However, a deviation from this trend was observed when the number of distributor holes was increased to 9. In this case, PCC production decreased to 37.15 grams. Visually, when the number of CO_2 gas distributor holes was increased from 3 to 6, the number of gas bubbles produced appeared to be greater, with the bubble sizes remaining similar between 3 and 6 holes. However, when the number of distributor holes was increased to 9, the resulting CO_2 gas bubbles were larger in size compared to those produced with 3 and 6 distributor holes, and their movement was noticeably slower. This phenomenon is likely attributed to the increased number of gas bubbles generated by the additional distributor holes, without corresponding control of the CO_2 gas pressure delivered from the gas cylinder to the reactor (see Figure 2). This condition resulted in a reduction in system pressure [22], which was visually observed during the experiment. The pressure drop was initiated by a lower reading on the pressure gauge (PG) located on the regulator along the gas outlet line to the reactor. Although the pressure drop was not highly significant, it was accompanied by a reduction in available gas

flow space due to the constant cross-sectional area of the reactor. These two factors contributed to the tendency of smaller bubbles exiting the distributor with 9 holes to coalesce, forming larger bubbles. This coalescence led to slower bubble movement within the liquid phase. The phenomenon of bubble coalescence and its effect on bubble velocity is illustrated in Figure 6. Consequently, the solubility of gas in the $\text{Ca}(\text{OH})_2$ solution decreased, as the total number of CO_2 bubbles decreased, and the resulting PCC product also decreased. According to Lefebvre *et al.* [23], the reaction could be accelerated if the gas bubble size was small, as smaller bubble sizes increased the interfacial area, thus enhancing the diffusion-reaction process.

In principle, a greater number of distributor holes increases the potential for more uniform CO_2 distribution throughout the liquid medium [24] compared to configurations with fewer holes, thereby enhancing gas-liquid interaction [25]. This condition promotes a more even reaction between CO_2 and $\text{Ca}(\text{OH})_2$ across the entire liquid-filled volume of the reactor. However, increasing the number of holes without maintaining a stable CO_2 pressure within the internal pipes can lead to a decrease in gas velocity and momentum. When the gas velocity becomes too low, the initially small CO_2 bubbles released from the distributor holes tend to coalesce into larger bubbles, as illustrated in Figure 6. This coalescence reduces the interfacial area, ultimately hindering the diffusion of CO_2 into the $\text{Ca}(\text{OH})_2$ solution.

Based on the data presented in Figures 3 and 5, a statistical analysis was conducted using one-way ANOVA test with three replications ($n = 3$) to evaluate the effects of CO_2 gas distributor holes. The results yielded p -values of 1.71×10^{-5} and 5.92×10^{-7} , respectively, both of which are less than the significance level ($\alpha = 0.05$). These findings indicate that both the CO_2 gas flow rate and the number of distributor holes have a statistically significant effect and play a critical role in CO_2 capture using $\text{Ca}(\text{OH})_2$, contributing to the formation of PCC [26]. This trend is closely associated with the positive influence of both parameters in enhancing turbulence and gas diffusion into the solution, thereby improving the gas-liquid contact and the interaction between CO_2 and the $\text{Ca}(\text{OH})_2$ solution during the reaction to form PCC.

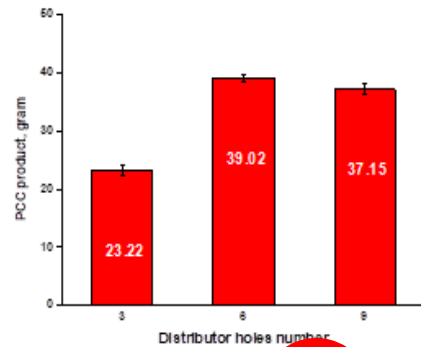


Figure 5: The effect of the number of CO_2 gas distributor holes with a CO_2 gas flow rate of 3 lpm.

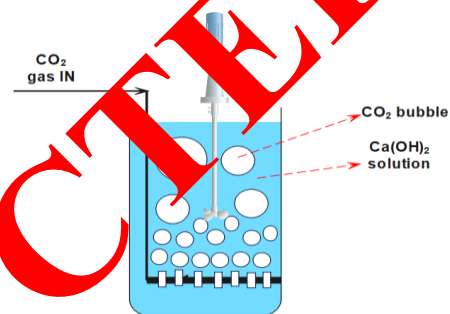


Figure 6: Illustration of small CO_2 gas bubbles forming a large bubble [1].

3.3 Results of product characterization testing

The PCC product obtained after 60 min of the CO_2 capture process was separated using filter paper, then dried in an oven at 110°C for 2 h. Once dried, the product was weighed to determine the mass of the resulting PCC using Equation (10). The PCC was then placed in a plastic bag and documented using a digital camera, without any modifications to its color or shape (see Figure 7). To ensure that PCC (CaCO_3) was formed and to identify the crystal types present, such as calcite, aragonite, vaterite, or a combination of these, this study employed FTIR and SEM analyses on the dried samples (see Figure 8) as well as on the raw material used ($\text{Ca}(\text{OH})_2$).

FTIR test results are shown in Figure 7. It could be seen that there was a significant change in the peaks of the raw material in Figure 8(a) and after being contacted with CO_2 gas in Figure 8(b). When compared with the FTIR test results of the PCC standard (CaCO_3) in Figure 9, the results were almost identical. Therefore, it could be confirmed that the product resulting from the reaction process was PCC.



Figure 7: PCC product obtained in this study.

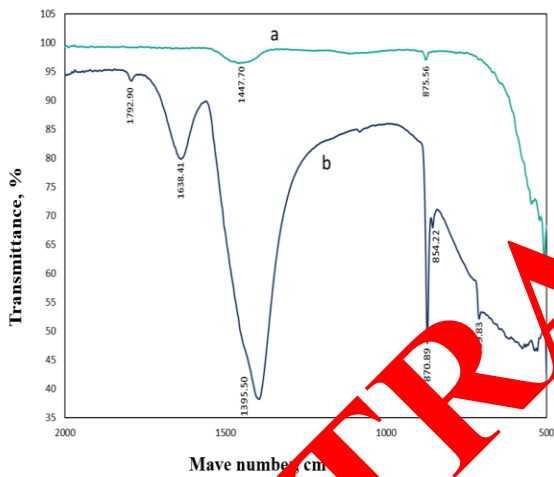


Figure 8: FTIR test results: a) raw material Ca(OH)_2 and b) PCC product from the reaction.

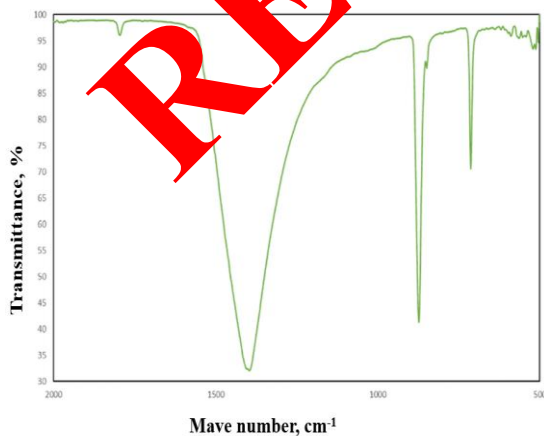


Figure 9: FTIR test results for standard PCC (CaCO_3) [16].

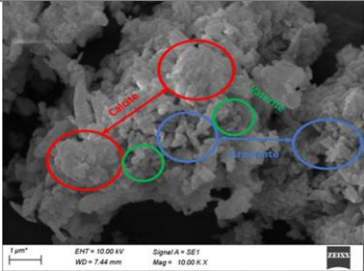
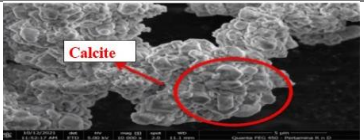
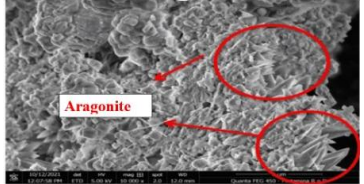
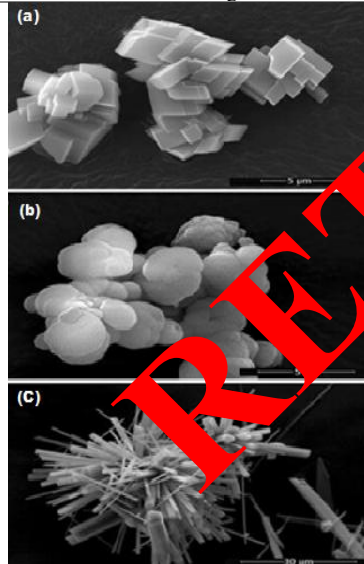
In addition to the FTIR test, an SEM test with a magnification of 10,000 times was also conducted to determine the type of PCC produced. According to the reviewed literature, calcite crystals typically exhibit a distinctive rhombohedral shape with layered surfaces [27], [28], vaterite appears as irregular spherical or globular aggregates [29], and aragonite has a needle-like or elongated prismatic structure [30], [31] (Table 2). Based on the SEM analysis conducted in this study and comparisons with Table 3 and relevant references [32], [33], as shown morphologically in Table 3, the results indicate that the PCC (CaCO_3) produced in this study consists of a mixed crystal composition comprising calcite, aragonite, and vaterite.

Table 2: Crystal types of PCC (CaCO_3)

Crystal Type	Morphology	Stability	Ref.
Calcite	Rhombohedral	Most stable	[27],[28],[34]
Vaterite	Spherical/globular	Metastable	[27],[28],[29]
Aragonite	Needle-like/prismatic	Stable under high pressure	[32], [33]

Based on the characterization results of the PCC produced in this study, the product was found to consist of a combination of three crystal forms: calcite, aragonite, and vaterite. The coexistence of these crystal types enables the formation of a more complex and versatile structure, suitable for a wide range of applications. For instance, vaterite, which exhibits a spherical or globular morphology with a high surface area, is highly suitable for cosmetic and pharmaceutical applications due to its excellent dispersion properties and high solubility [35]. Aragonite, characterized by its needle-like shape, can enhance mechanical properties when used as a reinforcing material in plastic or rubber composites [36]. Calcite, known for its stability and uniform particle size distribution, is ideal for use as a filler in the paper and plastic industries, providing structural strength and surface smoothness [37]. Therefore, the simultaneous presence of these three crystal forms in the PCC product offers performance advantages over conventional PCC, which typically consists of a single crystal phase (commonly calcite). These results suggest that the PCC produced in this study holds greater potential for application across various industrial sectors, including cosmetics, plastic fillers, and paper coatings.

Table 3: Comparison of SEM results with reference data.

SEM Result	Ref.
 <p>Calcite, vaterite, and aragonite</p>	This research
 <p>Calcite</p>	[32]
 <p>Aragonite</p>	
 <p>Calcite and aragonite</p>	[33]
<p>a) Calcite, b) Vaterite, and c) Aragonite</p>	

for commercial development. Moreover, the results can serve as a basis for decision-making in determining the next steps toward achieving a profitable and sustainable process system. In this study, the feasibility of the CO₂ capture process using Ca(OH)₂ absorbent was evaluated on a laboratory scale. The main cost components considered were raw materials (Ca(OH)₂ and CO₂ gas) and the energy required for stirring at 400 rpm. The price of Ca(OH)₂ with a concentration of 19.1% was \$0.031/L, based on pricing from CV. Kasugian Jaya, Indonesia. Calculations were based on a CO₂ flow rate of 3 L/min, a Ca(OH)₂ density of 1.1 g/cm³, a solution volume of 300 mL, a reaction time of 60 min, and a PCC product yield of 39.02 grams. The calculations were performed using Microsoft Excel. It was assumed that the CO₂ source incurs no cost (considered as a byproduct of an industrial process). The detailed cost and energy analysis results are presented in Table 4.

Table 4: Results of a rough simulation of the cost and energy analysis of the CO₂ capture process.

Components	Values
Ca(OH) ₂ solution volume	300 mL
Price of solution per liter	\$ 0.031
Electric consumption	0.05 kWh
Electric cost	\$ 0.0055
Total operational cost	\$ 0.0148
Yielded CaCO ₃ (PCC)	39.02 gram
CaCO ₃ (PCC) cost per gram	\$ 0.0148 / 39.02 gram = \$ 0.00038 /gram
Reaction conversion	45.84%

As shown in Table 4, the cost to synthesize 1 gram of CaCO₃ intended for pharmaceutical, cosmetic, or filler applications, this production cost remains economically viable, as the market price for premium-grade PCC is \$0.00052 per gram [38]. On the other hand, if the target is bulk-grade PCC with a market price of only \$0.00020 per gram [39], the synthesis method used in this study becomes unprofitable, resulting in a loss of \$0.00028 per gram. Moreover, if technical-grade CO₂ is used as a raw material, with a market price of \$0.46875 per liter (referring to the price from PT Gasindo Andalan Sukses, Cilegon – Indonesia.), the CO₂ capture process using Ca(OH)₂ to produce PCC is no longer feasible for commercial development, whether for bulk or premium-grade products. The calculated production cost in this scenario reaches \$2.163 per gram of PCC. Literature findings also suggest that CO₂ treatment remains economically impractical and is still associated with high operational costs [40].

3.4 Cost and energy analysis of the CO₂ capture process

Cost and energy analysis is an important aspect of any study, even if conducted as a preliminary estimation. Such analysis provides initial insights into whether the investigated process has the potential and feasibility

However, if the main objective is CO₂ emission mitigation to reduce the effects of global warming, and the PCC product is considered a byproduct rather than the primary goal, then this method may be considered a promising alternative technology. To ensure that the CO₂ capture process using Ca(OH)₂ absorbent is commercially viable, several conditions must be met. First, the PCC produced must meet premium-grade specifications according to its intended application, such as for pharmaceutical or cosmetic use. Second, further optimization is needed to improve reaction conversion and overall process efficiency. Lastly, the CO₂ source must be cost-free, ideally obtained directly from industrial flue gas that has undergone appropriate pre-treatment.

4 Conclusions

An increase in CO₂ gas flow rate can enhance the production of PCC, provided that it does not cause excessive turbulence that creates voids, which can hinder the diffusion of CO₂ into the Ca(OH)₂ solution. Excessive turbulence may also cause the Ca(OH)₂ suspension to rise and adhere to the reactor walls, negatively affecting the reaction. A similar phenomenon applies to the parameter of distributor hole number. Increasing the number of distributor holes without adequate control of CO₂ gas pressure may slow down gas movement within the Ca(OH)₂ solution due to the formation of larger bubbles through coalescence. This condition reduces the gas-liquid interfacial area, thereby decreasing the efficiency of the CO₂ and Ca(OH)₂ reaction to form PCC. In the variation of CO₂ flow rates at 2, 3, and 5 lpm, with the number of distributor holes fixed at 3, the resulting PCC yields were 12.1 grams, 23.22 grams, and 18.23 grams, respectively. It is evident that increasing the flow rate from 2 to 3 lpm resulted in a 92% increase in PCC production, while increasing it further to 5 lpm led to a 21.5% decrease. In another set of experiments, the number of distributor holes was varied at 3, 6, and 9, while maintaining a constant CO₂ flow rate of 3 lpm (identified as the optimal flow rate). The corresponding PCC yields were 23.22 grams, 39.02 grams, and 37.15 grams, respectively. Increasing the number of holes from 3 to 6 resulted in a 68% increase in PCC production, whereas increasing from 6 to 9 holes caused a slight decline of approximately 4.8%. Despite these fluctuations, statistical analysis using ANOVA confirmed that both the CO₂ flow rate and the number of distributor holes had a significant effect on PCC yield, with *p*-values of 1.71×10^{-5} and $5.92 \times$

10^{-7} , respectively (*p*-values < 0.05). These findings indicate that both parameters play a crucial role in the formation of PCC. Characterization of the PCC product using FTIR and SEM revealed that the synthesized PCC consists of a mixture of calcite and aragonite crystals, with a small presence of vaterite. This crystal composition broadens the potential applications of the product across various industries. To the best of the authors' knowledge, no previous studies have explicitly investigated the combined effects of CO₂ gas flow rate and the number of distributor holes on PCC synthesis using Ca(OH)₂-based CO₂ capture. Therefore, the findings of this study contribute meaningful insights to the existing body of research and support the further development of Carbon Capture, Utilization, and Storage (CCUS) as an alternative technology for greenhouse gas mitigation. The results may also serve as a basis for designing pilot and industrial scale reactors, particularly for PCC production targeting applications in the paper, plastic, and cosmetic industries, as well as other sectors identified in the cost and energy analysis. Further research is strongly recommended to explore more comprehensively the combined effects of distributor hole number and hole diameter. This is essential to determine whether increasing the number of holes beyond six, when combined with smaller hole sizes (below 0.2 cm), could improve or hinder PCC formation. A systematic investigation of these parameters is necessary to identify operational conditions that are effective, efficient, low-cost, and scalable for industrial applications. In addition, future studies should explore the use of CO₂ sourced from pretreated flue gas to assess the feasibility and readiness of the process for commercial-scale implementation.

Acknowledgements

The researcher extends sincere gratitude to the Department of Chemical Engineering of Universitas Sultan Ageng Tirtayasa and to the University itself for providing the facilities for the successful completion of this study. The findings of this study are expected to serve the public interest and foster further developments in scientific and technological fields.

Author Contributions

Nuryoto Nuryoto: Writing an original draft, Research concept and design, Data analysis and interpretation, Final approval of the article; Leli Rahmawati and

Herliza Julvita: Investigation, Collection and/or assembly of data; Rafiif Nur Tahta Bagaskara: Writing the article and editing.

Conflicts of Interest

The authors declare no conflict of interest.

References

- [1] O. Levenspiel, *Chemical Reaction Engineering*, 3rd ed., New York: John Wiley & Sons, 1999.
- [2] H. Kierzkowska-Pawlak, "Determination of kinetics in gas-liquid reaction systems. An overview," *Ecological Chemistry and Engineering S*, vol. 19, no. 2, pp. 175–196, Jun. 2012, doi: 10.2478/v10216-011-0014-y.
- [3] D. Behvandi, M. Arefizadeh, A. Ghaemi, and S. Shahhosseini, "Evaluation of diffusion and Henry's coefficients of CO₂ absorption using response surface methodology and artificial neural network models," *Case Studies in Chemical and Environmental Engineering*, vol. 9, Jun. 2024, Art. no. 100723, doi: 10.1016/j.cscee.2024.100723.
- [4] M. Mutailipu, Y. Song, Q. Yao, Y. Liu, and J. M. Trusler, "Solubility and interfacial tension models for CO₂-brine systems under CO₂ geological storage conditions," *Fuel*, vol. 367, Feb. 2024, Art. no. 129712, doi: 10.1016/j.fuel.2023.129712.
- [5] A. N. Conejo, "Physical and mathematical modelling of mass transfer in lactose due to bottom gas stirring: A review," *Processes*, vol. 8, no. 7, pp. 1–23, Jun. 2020, Art. no. 750, doi: 10.3390/pr8070750.
- [6] M. H. C. Smith, M. M. V. Ness, Abbott, and M. T. Swihart, *Introduction to Chemical Engineering Thermodynamics*, 8th ed., New York: McGraw-Hill Education, 2018.
- [7] B. Dollet, "Coarsening of foams driven by concentration gradients of gases of different solubilities," *Langmuir*, vol. 39, no. 45, pp. 16174–16181, Nov. 2023, doi: 10.1021/acs.langmuir.3c02533.
- [8] M. N. Kashid, A. Renken, and L. Kiwi-Minsker, "Gas-liquid and liquid-liquid mass transfer in microstructured reactors," *Chemical Engineering Science*, vol. 66, no. 17, pp. 3876–3897, Nov. 2011, doi: 10.1016/j.ces.2011.05.015.
- [9] N. Nuryoto, M. H. Alfarizi, M. A. S. Kelana, and R. N. T. Bagaskara, "Alternative technology towards clean and sustainable industry: Conversion of carbon dioxide gas into potassium carbonate," *Advances in Science and Technology Research Journal*, vol. 19, no. 4, pp. 183–197, Feb. 2025, doi: 10.12913/22998624/200561.
- [10] E. Sari et al., "Synthesis of precipitated calcium carbonate with the addition of aloe vera extract under different reaction temperatures," *International Journal of Applied Science and Engineering*, vol. 20, no. 1, pp. 1–7, Mar. 2023, doi: 10.6703/IJASE.202303_20(1).007.
- [11] N. Erdogan and H. A. Erk, "Precipitated calcium carbonate production, synthesis and properties," *Physicochemical Problems of Mineral Processing*, vol. 53, no. 1, pp. 57–68, Jan. 2017, doi: 10.1007/s10170105.
- [12] M. A. Baqiyah et al., "Precipitation process of CaCO₃ from natural limestone for functional materials," *Journal of AOAC International*, vol. 103, no. 2, Apr. 2020, doi: 10.5740/jaoacint.19-0356.
- [13] T. Tiefenthaler and M. Mazzotti, "Experimental investigation of a continuous reactor for CO₂ capture and CaCO₃ precipitation," *Frontiers in Chemical Engineering*, vol. 4, Feb. 2022, Art. no. 830284, doi: 10.3389/fceng.2022.830284.
- [14] P. Ochonma, X. Gao, and G. Gadikota, "Tuning reactive crystallization pathways for integrated CO₂ capture, conversion, and storage via mineralization," *Accounts of chemical research*, vol. 57, no. 3, pp. 267–274, Jan. 2024, doi: 10.1021/acs.accounts.3c00482.
- [15] V. Bortuzzo, S. Bertagna, L. Braidotti, and V. Bucci, "Towards CO₂ emissions reduction of shipping: Ca(OH)₂ based carbon capture system for safeguarding the marine environment," *Frontiers in Marine Science*, vol. 12, Feb. 2025, Art. no. 1434342, doi: 10.3389/fmars.2025.1434342.
- [16] Nuryoto, H. Heriyanto, L. Rahmawati, and H. Julvita, "Transforming greenhouse gases: CO₂ conversion into high-value precipitated calcium carbonate (pcc) (original title: Transformasi gas rumah kaca: Mengubah CO₂ menjadi bahan bernilai tinggi berupa precipitated calcium carbonate (pcc))," *Jurnal Sains dan Teknologi*, vol. 23, no. 2, pp. 205–216, Jul. 2024, doi: 10.23887/jstundiksha.v13i2.79553.
- [17] N. Zhenqi, G. Yincheng, and L. Wenyi, "Experimental studies on CO₂ capture in a spray scrubber using NaOH solution," presented at the International Conference on Energy and

- Environment Technology, Guilin, China, Oct. 16–18, 2009.
- [18] M. Bagi, M. V. Razlighi, M. Shanbedi, and A. Karim, “A comprehensive parametric study on CO₂ removal from natural gas by hollow fiber membrane contactor: A computational fluid dynamics approach,” *Chemical Engineering & Technology*, vol. 47, no. 4, pp. 732–738, Feb. 2024, doi: 10.1002/ceat.202300504.
- [19] Y. Ihsana, P. A. Rama, R. Puspita, S. Winardi, and T. Nurtono, “Bubble column application on purification of biogas and production of nano-calcium carbonate in continuous process,” *Malaysian Journal of Fundamental and Applied Sciences*, vol. 16, no. 3, pp. 286–291, Jun. 2020, doi: 10.11113/mjfas.v16n3.1567.
- [20] Y. Wang et al., “Investigation of mass transfer characteristics under turbulent condition in adsorption separation process for CO₂ capture,” *Journal of Environmental Chemical Engineering*, vol. 10, no. 1, Jan. 2022, Art. no. 107106, doi: 10.1016/j.jece.2021.107106.
- [21] Q. Wehrung et al., “Impact of operational parameters on the CO₂ absorption rate in Ca(OH)₂ aqueous carbonation—implications for process efficiency,” *Energy & Fuels*, vol. 38, no. 17, pp. 16678–16691, Aug. 2024, doi: 10.1021/acs.energyfuels.4c0245.
- [22] F. Bai and Y. Lu, “Effects of impurities on anthropogenic CO₂ pipeline transport,” *Energy & Fuels*, vol. 38, no. 5, pp. 9958–9966, May 2024, doi: 10.1021/acs.energyfuels.4c00935.
- [23] J. Lefebvre, S. Bjoehr, and T. Gomb, “Modeling of the transient behavior of a slurry bubble column reactor for CO₂ methanation, and comparison with a tube bundle reactor,” *Renewable Energy*, vol. 151, pp. 118–136, May 2020, doi: 10.1016/j.renene.2019.11.008.
- [24] X. Li, A. Nyngfelt, D. Pallares, C. Linderholm, and T. Mattisson, “Investigation on the performance of volatile distributors with different configurations under different fluidization regimes,” *Energy & Fuels*, vol. 36, no. 17, pp. 9571–9587, Jan. 2022, doi: 10.1021/acs.energyfuels.1c04159.
- [25] B. H. Kim, J. H. Kim, P. S. Kang, S. K. Yoo, H. C. Yoo, and E. S. Lee, “Gas distributor for removing carbon dioxide through head pressing,” South Korea Patent, KR101140774B, Jul. 02, 2012.
- [26] I. K. Rind, A. Sari, M. Tuzen, M. F. Lanjwani, and T. A. Saleh, “Development of fly ash/melamine composites for crystal violet dye removal from aqueous media,” *Environmental Nanotechnology, Monitoring & Management*, vol. 23, Jun. 2025, Art. no. 101056, doi: 10.1016/j.enmm.2025.101056.
- [27] L. Minkowicz, A. Dagan, V. Uvarov, and O. Benny, “Controlling calcium carbonate particle morphology, size, and molecular order using silicate,” *Materials*, vol. 14, no. 13, Jun. 2021, Art. no. 3525, doi: 10.3390/ma14133525.
- [28] R. A. Boulos, F. Zhang, E. S. Tjandra, A. D. Martin, D. Spagnoli, and C. L. Raston, “Spinning up the polymorphs of calcium carbonate,” *Scientific Reports*, vol. 4, Jan. 2014, Art. no. 3616, doi: 10.1038/srep03616.
- [29] R. Febrida et al., “Synthesis and characterization of porous CaCO₃ vaterite particles by simple solution method,” *Materials*, vol. 14, no. 16, Aug. 2021, Art. no. 4425, doi: 10.3390/ma14164425.
- [30] E. Benny, T. Shahwan, and M. Tanoğlu, “Morpho-synthesis of CaCO₃ at different reaction temperatures and the effects of PDDA, CTAB, and EDTA on the particle morphology and polymorph stability,” *Powder Technology*, vol. 170, no. 3, pp. 194–202, Sept. 2007, doi: 10.1016/j.powtec.2007.05.004.
- [31] W. Nagaki, N. Doki, M. Yokota, K. Yamashita, T. Kojima, and T. Tanaka, “Control of crystal size and morphology of calcium carbonate crystal polymorphism,” *Journal of Materials Science and Chemical Engineering*, vol. 9, no. 4, pp. 38–45, Apr. 2021, doi: 10.4236/msce.2021.94005.
- [32] N. Naldi, S. Arief, R. Desmiarti, E. Sari, and E. R. Desfitri, “Removal of chlorine content in precipitated calcium carbonate (pcc) through washing and filtration processes (original title: Penghilangan kadar klorine pada precipitate calcium carbonate (pcc) dengan proses pencucian dan filtrasi,” *Eksergi*, vol. 20, no. 3, pp. 200–209, Nov. 2023, doi: 10.31315/e.v20i3.9684.
- [33] R. Ševčík, P. Šašek, and A. Viani, “Physical and nanomechanical properties of the synthetic anhydrous crystalline CaCO₃ polymorphs: Vaterite, aragonite and calcite,” *Journal of materials science*, vol. 53, no. 6, pp. 4022–4033, Dec. 2018, doi: 10.1007/s10853-017-1884-x.
- [34] L. Pastero, E. Costa, M. Bruno, M. Rubbo, G. Sgualdino, and D. Aquilano, “Morphology of calcite (CaCO₃) crystals growing from aqueous solutions in the presence of Li⁺ ions. Surface behavior of the {0001} form,” *Crystal growth &*



- design*, vol. 4, no. 3, pp. 485–490, Mar. 2004, doi: 10.1021/cg034217r.
- [35] B. Zafar, J. Campbell, J. Cooke, A. G. Skirtach, and D. Volodkin, “Modification of surfaces with vaterite CaCO_3 particles,” *Micromachines*, vol. 13, no. 3, p. 473, Mar. 2022, doi: 10.3390/mi13030473.
- [36] S. G. Lyu, S. Park, and G. S. Sur, “The synthesis of vaterite and physical properties of PP/ CaCO_3 composites,” *Korean Journal of Chemical Engineering*, vol. 16, no. 4, pp. 538–542, Jul. 1999, doi: 10.1007/BF02698281.
- [37] T. Enomae and K. Tsujino, “Application of spherical hollow calcium carbonate particles as filler and coating pigment,” *TAPPI Journal*, vol. 3, no. 6, pp. 493–493, Jun. 2004.
- [38] Pucement resource. “Calcium carbonate price trend and forecast: Calcium carbonate regional price overview.” [procurementresource.com](https://www.procurementresource.com/resource-center/calcium-carbonate-price-trends). Accessed: Jul. 18, 2025. [Online]. Available: <https://www.procurementresource.com/resource-center/calcium-carbonate-price-trends>
- [39] Made in china. “Calcium carbonate price pcc.” [made-in-china.com](https://www.made-in-china.com/price/prodetail_Carbonate). Accessed: Jul. 18, 2025. [Online]. Available: https://www.made-in-china.com/price/prodetail_Carbonate
- [40] I. Raheem et al., “A comprehensive review of approaches in carbon capture, storage, and utilization to reduce greenhouse gases,” *Applied Science and Engineering Progress*, vol. 19, no. 2, Apr. 2025, Art. no. 7629, doi: 10.14416/j.asep.2024.11.004.

RETRACTED